Supporting Information: Second-order NonLinear Optical Properties of X-Shaped Pyrazine Derivatives

Verònica Postils,*,† Zuzana Burešová,‡ David Casanova,¶,§ Benoît Champagne,‖ Filip Bureš,‡ Vincent Rodriguez,*,† and Frédéric Castet*,†

†*Univ. Bordeaux, CNRS, Bordeaux INP, Institut des Sciences Moléculaires, UMR 5255, F-33400 Talence, France*

‡*Institute of Organic Chemistry and Technology, Faculty of Chemical Technology, University of Pardubice, Studentská 573, Pardubice 532 10, Czech Republic*

¶*Donostia International Physics Center (DIPC), Manuel Lardizabal Ibilbidea 4, 20018 Donostia, Euskadi, Spain*

§*Ikerbasque Foundation for Science, Plaza Euskadi 5, 48009 Bilbao, Euskadi, Spain*

‖*Unité de Chimie Physique Théorique et Structurale, Chemistry Department, Namur Institute of Structured Matter, University of Namur, Belgium*

E-mail: vpostils@gmail.com; vincent.rodriguez@u-bordeaux.fr; frederic.castet@u-bordeaux.fr

Contents

S1 Synthesis of compound 2D

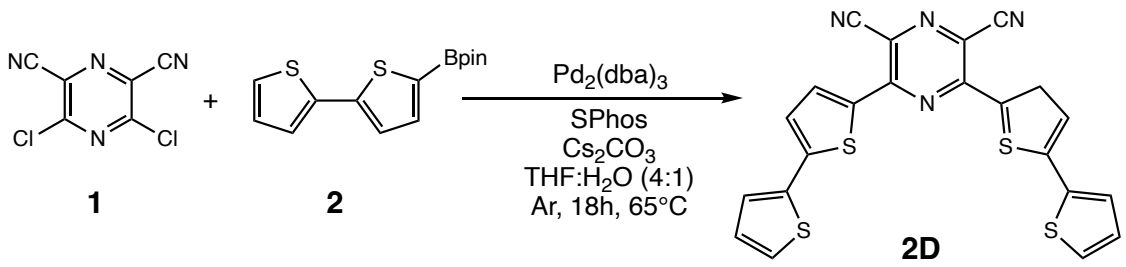

Figure S1: Synthesis of compound **2D**.

In a Schlenk flask, 3,5-dichloropyrazine-2,6-dicarbonitrile **1** (199 mg, 1.0 mmol) and pinacol ester **2** (347 mg, 2.1 mmol) were dissolved in the mixture of THF/H_2O (40 ml, 4:1). Argon was bubbled through the solution for 10 min, after that $Pd_2(dba)_3$ (46 mg, 0.005 mmol, 5%), SPhos (21 mg, 0.005 mmol, 5%), and Cs_2CO_3 (680 mg, 2.1 mmol) were added. The resulting reaction mixture was stirred at 65 °C for 18 h (Figure S1). The reaction mixture was diluted with water (20 ml) and extracted with DCM (3 x 20 ml). The combined organic extracts were dried over anhydrous Na_2SO_4, the solvents were evaporated *in vacuo*, and the crude product was purified by column chromatography (SiO_2, DCM:Hex 2:1) and subsequent crystallization from 1,2-dichloroethane/hexane. Compound **2D** is red solid (213 mg, 47 %); mp = 295 °C.

^{1}H NMR (25 °C, 500 MHz, d_6-DMSO): δ = 8.29 (d, J = 4Hz, 2H), 7.74 (d, J = 5Hz, 2H), 7.66 (d, J = 3.5Hz, 2H), 7.62 (d, J = 4Hz, 2H), 7.21 (t, J = 4Hz, 2H) ppm. **^{13}C NMR** (25 °C, 125 MHz, d_6-DMSO): δ = 149.10, 145.59, 135.52, 135.10, 133.17, 129.05, 128.44, 126.99, 126.51, 119.66, 116.12 ppm. **HR-FT-MALDI-MS** (DCTB) m/z calcd. for $C_{22}H_{10}N_4S_4^+$ $(M)^+$ 457.97828; found 457.97824.

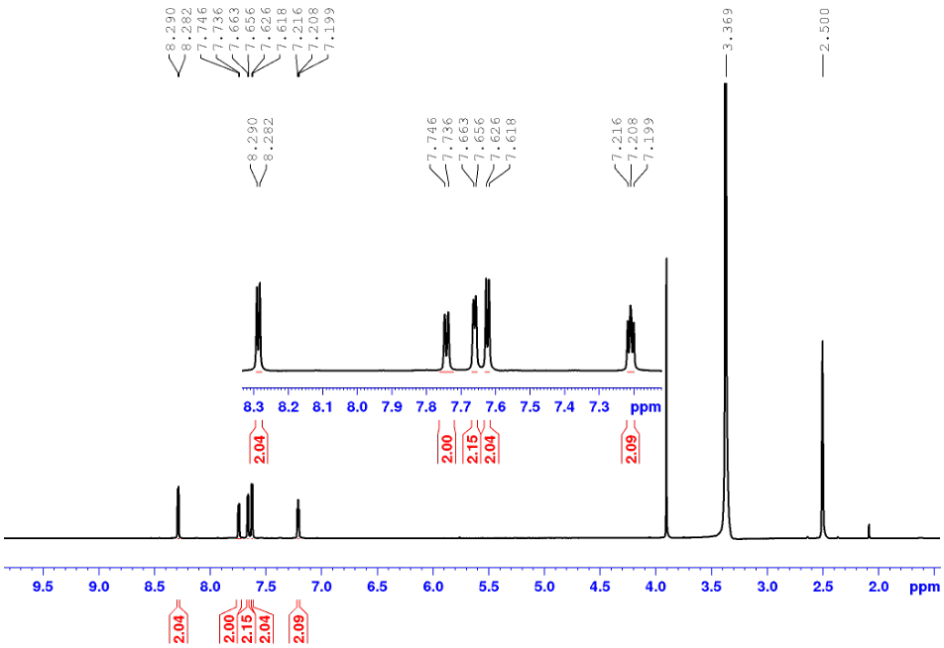

Figure S2: ^{1}H NMR spectrum of compound **2D**.

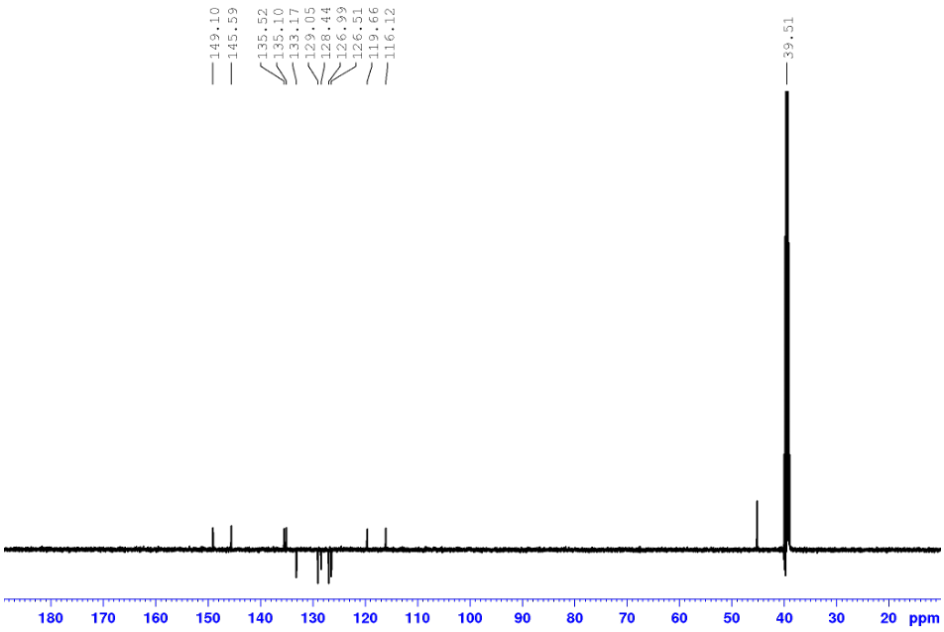

Figure S3: ^{13}C NMR spectrum of compound **2D**.

S2 HRS experiments

S2.1 Scaling the quadratic dependence of the HRS Signal through power scans

The HRS amplitudes have first been obtained by performing power scans, *i.e.* by determining the coefficient of the quadratic dependence of the scattered intensity as a function of the incident intensity and for different solute concentrations (equation 1). The polarization configuration was set to vertical-vertical (VV), *i.e.* with vertically polarized incident light ($\Psi = 90°$) and scattered light analyzed vertically. Power scans were performed on diluted solutions at different concentrations (varying from 10^{-4} M to 1.5×10^{-2} M depending on the NLO response of each compound). All experiments were carried out at room temperature. Each data point of the power scan was an average of 3 accumulations with an acquisition time of 20 s at 1064 nm and 30 s at 1300 nm to achieve a good signal-to-noise ratio, depending on the solution and excitation wavelength. The coefficient of quadratic dependence was obtained by fitting the power curves (see Figures S4 and S5) as a function of incident power (I_ω) and solute concentration (C_X) using a custom-built 2D fitting function of the form:

$$I_{2\omega}^{\Psi V} = (p_1 + p_2 C_X)(I_\omega - p_3)^2 \tag{S1}$$

where p_i (i = 1–3) are (all positive) fitting parameters. The extracted quantity is $C_{VV}\beta^2 = R.p_2/p_1$, where $R = [C\beta^2 C_{\Psi V}]_S = 6088$ a.u. is the chloroform contribution, used as the internal reference and assumed constant at both 1064 nm and 1300 nm wavelengths.

S2.2 Quantifying the dipolar/octupolar character of the HRS Response through polarization scans

The depolarization ratios (DR) were obtained by performing polarization scans, *i.e.* through stepwise variation of the incident light linear plane of polarization, at constant incident

power. The scattered intensity of the binary solution was measured for the pure solvent, and for the most concentrated binary solution to extract the chromophore contribution (Eq. 2). The polarization configuration was set to Ψ-V (where Ψ is the variable angle of the half-wave plate) for the incident and scattered lights, respectively. Polarization scans were performed between 0° and 180° in 5° steps. All experiments were carried out at room temperature. Each data point of the polarization scan was an average of three accumulations with an acquisition time of 20 s (1300 nm) or 30 s (1600 nm) each. The DR values were determined by fitting the polarization curves (see Figures S4 and S5) using a constrained custom-built fitting function of the form:

$$I_{2\omega}^{\Psi V} = A(\cos^4(\Psi - \Psi_0) + (1 + DR_i)\cos^2(\Psi - \Psi_0)\sin^2(\Psi - \Psi_0) + DR_i \sin^4(\Psi - \Psi_0)) \quad \text{(S2)}$$

where the intensity factor A, the angular offset Ψ_0 and the depolarization ratio DR_i are fitting parameters.

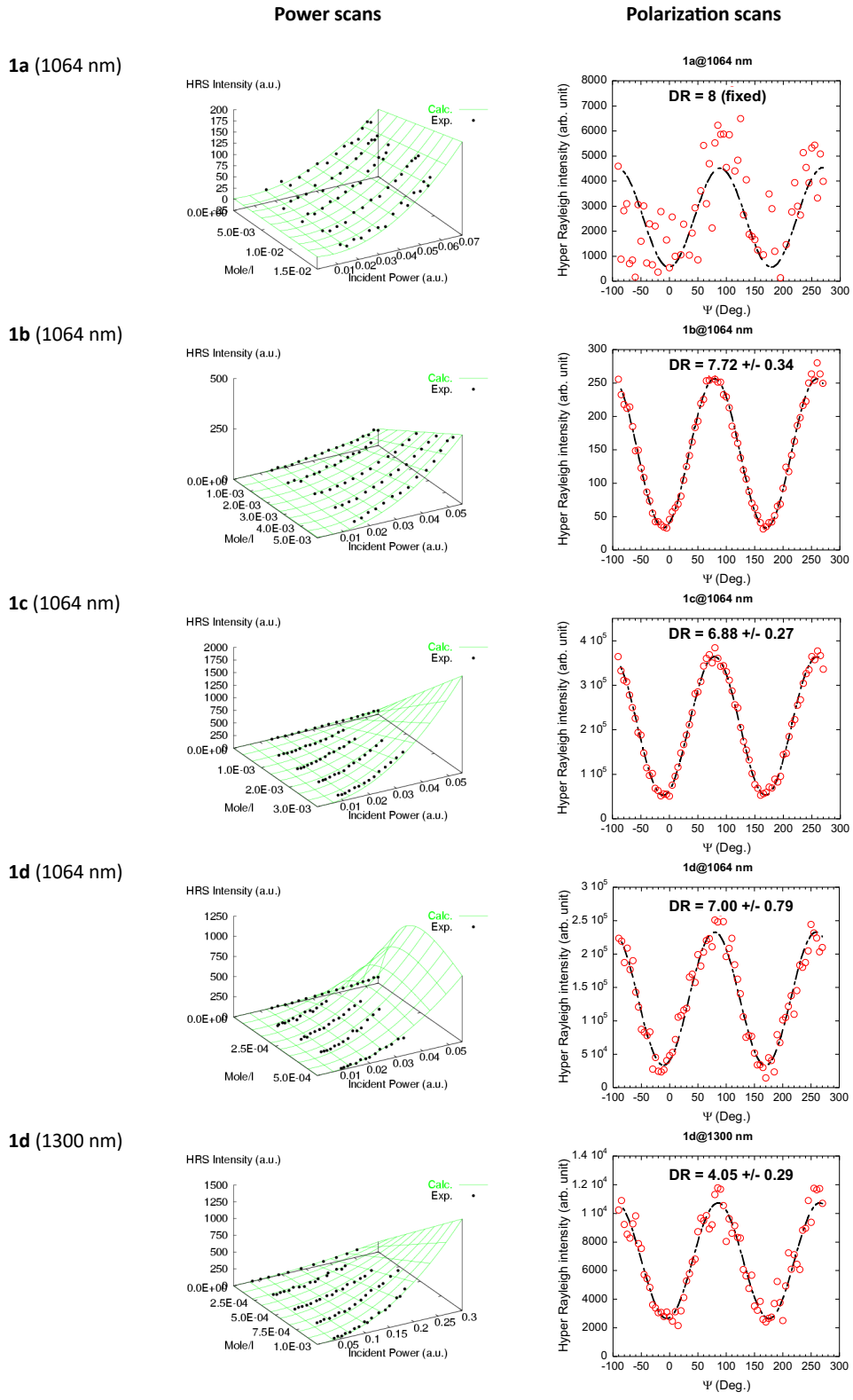

Figure S4: HRS power and polarization scans for derivatives of Family **1**.

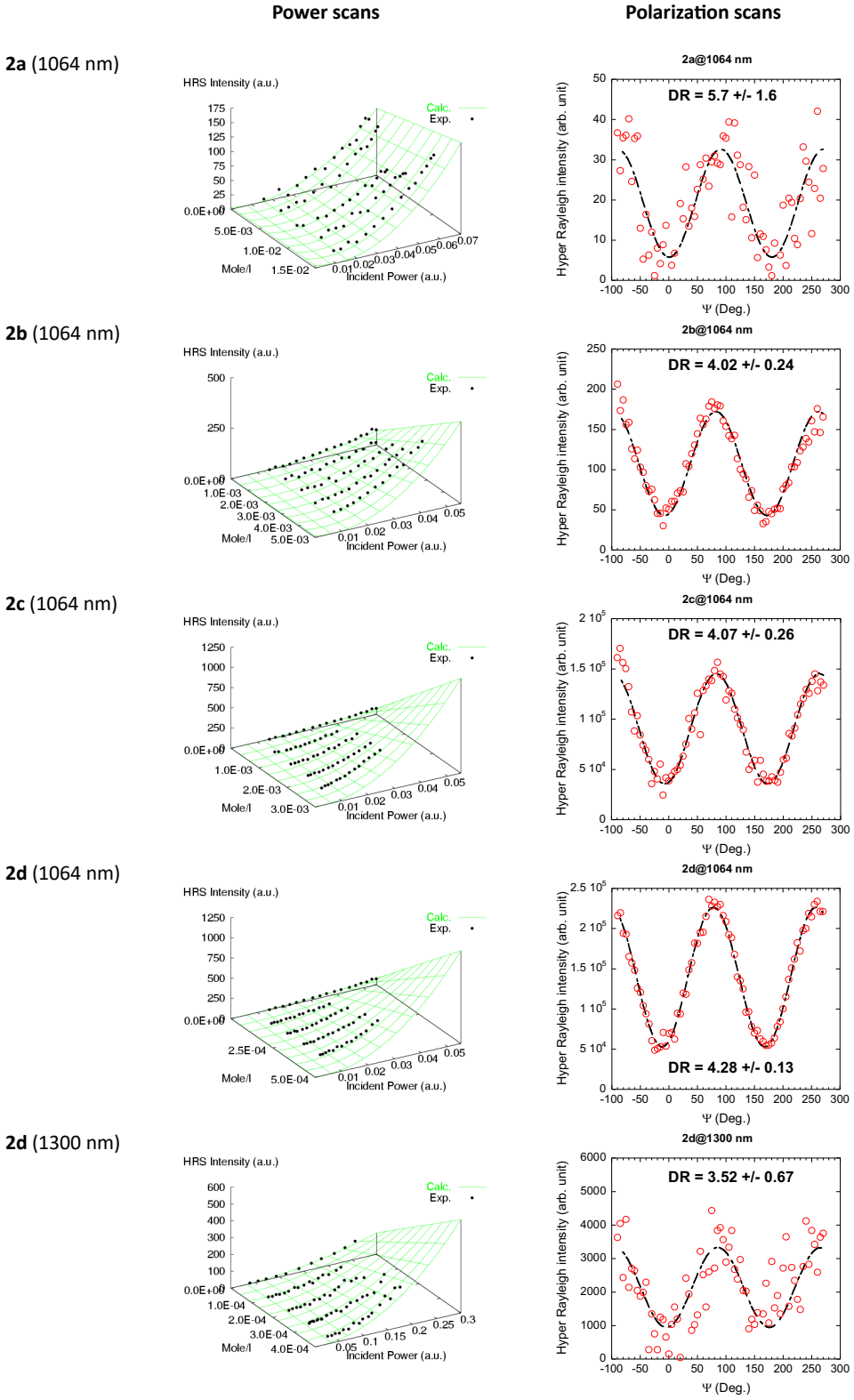

Figure S5: HRS power and polarization scans for derivatives of Family **2**.

S3 Thermodynamic Analyses

Table S1 presents all the conformational isomers characterized for the studied chromophores, together with structural details, relative energies, and Boltzmann statistical weights at room temperature. The later have been computed according to the standard expressions:

$$p_i = \frac{1}{Z} \exp\left(\frac{-\Delta G_i^\circ}{k_B T}\right) \qquad ; \qquad Z = \sum_{j=1} \exp\left(\frac{-\Delta G_j^\circ}{k_B T}\right) \tag{S3}$$

where i is the conformer of interest, ΔG_i° and ΔG_j° are the relative Gibbs energies of states i and j, respectively, k_B is the Boltzmann constant, T refers to the assumed room temperature of 298.15K, and Z is the canonical partition function. Z acts as a normalization denominator that constrains the probabilities of all considered conformers j to add up to 1. Only conformers with general probabilities higher than 0.05 (5.0%) (*i.e.*, $\Delta G^\circ < 1.65$ kcal·mol^{-1} with respect to the most stable species) have been taken into account in the calculation of optical properties. When relevant, Boltzmann probabilities were recomputed limiting the considered conformers j to these ones.

In Table S1, the allocated molecular point groups are exact, or have been attributed within an error lower than 0.01Å, following Equation S4.[S1] Molecules that do not belong to an exact point group but fulfill the last condition are designated with an asterisk.

$$\text{error} = \frac{1}{n} \sum_{i=1}^{n} \max_j \frac{\left|\mathrm{A}_j^i - \mathrm{B}_j^i\right|}{r_j} \tag{S4}$$

Equation S4 provides the error associated with a given symmetry element (*i.e.*, an axis or a plane), while i refers to the i^{th} symmetry operation associated within that element. Each atom of the molecule (A_j) is defined within a symmetry operation (A_j^i) and related through

Table S1: Point group, structural parameters (ϕ_n, degrees), and relative Gibbs energies (ΔG, kcalmol^{-1}) of all the various conformational isomers of each chromophore. Dihedral angles ϕ_n are defined on chromophore **2E** in Figure S6. Boltzmann probabilities are computed using Equation S3. (Considered) probabilities are re-scaled values considering only isomer with (General) probabilities >5.0%.

Compound	Point Group	Structural Parameters	$\Delta G^{(1)}$	Boltzmann Probability	
		ϕ_1, ϕ_3, (ϕ_5) / ϕ_2, ϕ_4, (ϕ_6)		(General)	(Considered)
1A-(c)	C2v	(0.00) / (0.00)	3.31		–
2A-(c)	C2v	(0.00) / (0.00)	0.00		–
1B-c	C2*	-25.42 / -25.30	4.61 (0.00)	84.9	87.9
1B-t-c	C1	29.05 / -142.67	5.78 (1.17)	11.7	12.1
1B-t	C1	-147.35 / -124.08	6.52 (1.91)	3.4	–
2B-c	C2*	3.90 / 3.89	0.00	48.3	67.9[(2)]
2B-t-c	CS	180.00 / 0.00	0.24	32.1	32.1
2B-c'	C2	0.00 / 0.00	0.53	19.6	–
1C-c(t)	C2*	19.38; (-179.49) / 19.42; (-179.50)	6.31 (0.00)	74.7	75.5
1C-c(c)	C2*	-19.44; (1.73) / -18.43; (1.71)	6.98 (0.67)	24.2	24.5
1C-t(t)	C1	-142.97; (179.99) / -134.44; (178.83)	8.92 (2.61)	0.9	–
1C-t(c)	C2*	-139.86; (1.75) / -139.83; (1.75)	9.89 (3.58)	0.2	–
2C-c(t)	C2v	0.00; (180.00) / 0.00; (180.00)	0.00	91.4	91.4
2C-c(c)	C2v*	0.01; (0.00) / 0.01; (0.00)	1.40	8.5	8.6
2C-t(t)	C2	-178.54; (-179.86) / -178.54; (-179.86)	4.64	0.04	–
2C-t(c)	C2	178.51; (-0.26) / 178.51; (-0.26)	5.59	0.01	–
1D-ct	C2	-22.39; 157.54 / -22.39; 157.54	6.35 (0.00)	71.2	72.4
1D-cc	C2	23.54; 29.34 / 23.54; 29.34	7.30 (0.95)	14.3	14.5
1D-tt-ct	C1	143.20; -154.58 / -26.67; 156.73	7.36 (1.01)	12.8	13.1
1D-tc	C1	28.07; -30.28 / -144.34; -29.81	8.58 (2.23)	1.7	–
2D-ct	CS*	-1.83; -157.35 / 1.75; 157.36	0.00	98.6	100.0
2D-cc	C2	3.08; -27.66 / 3.08; -27.66	2.55	1.3	–
2D-tt	C2*	176.02; -156.79 / 176.02; -156.80	4.19	0.1	–
2D-tc	C1	-179.79; -28.43 / 175.93; 29.36	6.03	0.004	–
1E-ct(t)	C2	-21.08; 163.14; (-179.52) / -21.08; 163.14; (-179.52)	4.71 (0.00)	87.6	91.9
1E-tt(t)	C1	-25.36; 160.74; (-178.97) / 143.71; -157.64; (179.39)	6.15 (1.44)	7.7	8.1
1E-cc(t)	C2	22.51; 27.30; (179.57) / 22.51; 27.30; (179.57)	6.80 (2.08)	2.6	–
1E-ct(c)	C2	-21.11; 162.55; (-2.29) / -21.11; 1622.55; (-2.29)	7.20 (2.49)	1.3	–
1E-cc(c)	C2	21.64; 25.06; (-0.20) / 21.64; 25.06; (-0.20)	7.75 (3.03)	0.5	–
1E-ct(c)-tt(c)	C1	143.58; -158.52; (2.05) / -25.19; 160.81; (-1.74)	8.36 (3.65)	0.2	–
2E-ct(t)	C2*	1.96; -160.59; (179.50) / 1.96; -160.60; (179.49)	0.00	72.9	74.0
2E-ct(c)	CS*	-1.36; -163.48; (0.99) / 1.36; 163.48; (-0.99)	0.81	18.7	19.0
2E-cc(t)	C2	2.34; -24.99; (-179.44) / 2.34; -24.99; (-179.44)	1.39	6.9	7.0
2E-tt(t)	C2	176.67; -160.04; (179.75) / 176.67; -160.04; (179.75)	2.50	1.1	–
2E-cc(c)	C2*	-1.43; -24.88; (-3.00) / -1.43; -24.88; (-3.00)	3.27	0.3	–
2E-tt(c)	C2	177.42; -159.97; (2.54) / 177.42; -159.97; (2.54)	5.20	0.01	–

[(1)] Relative Gibbs energies are given considering the conformers of both families. Relative energy values calculated considering only Family 1 are given in parenthesis.

* Symmetry is not exactly fulfilled, but it presents a deviation lower than 0.01Å in Equation S4.

[(2)] Probability value exceptionally computed as the sum of the probabilities of the two cis isomers (2B-c and 2B-c'), which are isoenergetic in terms of electronic energy.

that operation to the closest atom of the same type (B_j^i). The numerator is the distance that the generated atom lies from one of its symmetry-equivalent counterparts. The denominator r_j is the perpendicular distance between the atom A_j and the symmetry element, and it serves to keep the error independent of the molecule's size. n is the order of the symmetry element.

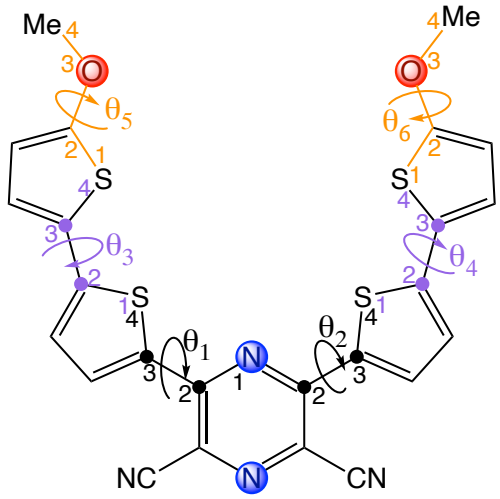

Figure S6: **2E** compound holding the definition of the dihedral angles used in Table S1.

S4 Absorption properties and characterization of the excited states

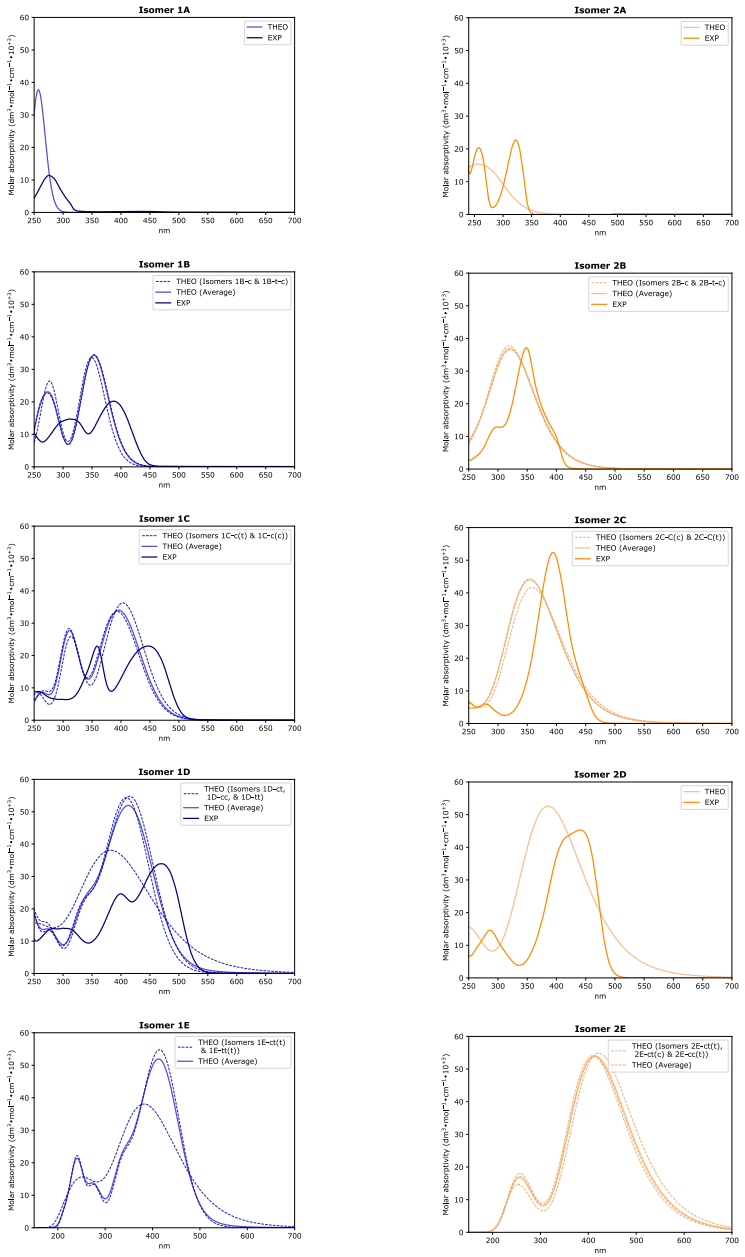

Figure S7: Experimental and computated UV-Vis spectra of 2,3- (left) and 2,6- (right) isomers. Theoretical results were obtained at the IEF-PCM/M06-2X(D3)/6-311+G(d) level of theory in chloroform and using a Gaussian broadening of the absorption peaks with a half-width at half-maximum (HWHM) of 0.25 eV.

Table S2: Wavelengths (λ_{ge}, nm), energies (ΔE_{ge}, eV), squared transition dipoles (μ^2_{ge}, a.u.^{2}), oscillator strengths (f_{ge}), dipole moment differences ($\Delta\mu_{ge}$, a.u.), and weights of the main electronic excitations (>5%) computed at the IEF-PCM/M06-2X/6-311G(d) level in chloroform for the lowest-energy optical transitions of the various conformers populated at room temperature.

Comp.	Transition	λ_{ge}	ΔE_{ge}	μ^2_{ge}	f_{ge}	$\Delta\mu_{ge}$	Electronic excitations
1A-(c)	$S_0 \rightarrow S_1$	259	4.79	3.40	0.398	3.865	98% H→L
	$S_0 \rightarrow S_2$	255	4.86	2.60	0.310	0.998	96% H→L+1
	$S_0 \rightarrow S_3$	239	5.19	0.02	0.002	0.746	96% H-1→L+1
2A-(c)	$S_0 \rightarrow S_1$	280	4.43	3.77	0.409	0.836	97% H→L
	$S_0 \rightarrow S_2$	264	4.69	0.02	0.003	0.656	87% H-1→L, 8% H-4→L
	$S_0 \rightarrow S_3$	239	5.18	3.42	0.435	0.223	96% H→L+1
1B-c	$S_0 \rightarrow S_1$	363	3.41	4.21	0.352	5.829	96% H→L
	$S_0 \rightarrow S_2$	345	3.60	3.99	0.352	5.671	97% H→L+1
	$S_0 \rightarrow S_3$	297	4.18	0.07	0.007	0.600	71% H-4→L+1, 17% H-3→L+1
	$S_0 \rightarrow S_4$	284	4.37	1.92	0.205	5.949	62% H-1→L, 17% H-4→L
1B-t-c	$S_0 \rightarrow S_1$	357	3.48	3.60	0.307	6.398	94% H→L
	$S_0 \rightarrow S_2$	343	3.61	3.95	0.349	6.218	96% H→L+1
	$S_0 \rightarrow S_3$	298	4.17	0.07	0.007	0.702	72% H-4→L+1, 7% H-3→L+1, 6% H-2→L+1
2B-c	$S_0 \rightarrow S_1$	330	3.76	5.93	0.546	2.490	94% H→L+1
	$S_0 \rightarrow S_2$	325	3.82	5.64	0.528	2.485	92% H→L
	$S_0 \rightarrow S_3$	311	3.99	2.59	0.253	5.755	89% H-1→L
2B-t-c	$S_0 \rightarrow S_1$	330	3.76	5.93	0.546	2.443	95% H→L+1
	$S_0 \rightarrow S_2$	322	3.85	5.14	0.486	2.437	90% H→L, 5% H-1→L+1
	$S_0 \rightarrow S_3$	308	4.02	3.71	0.366	5.438	91% H-1→L
1C-c(t)	$S_0 \rightarrow S_1$	412	3.01	5.32	0.392	6.193	95% H→L
	$S_0 \rightarrow S_2$	376	3.30	4.80	0.388	6.122	97% H→L+1
	$S_0 \rightarrow S_3$	311	3.98	4.76	0.464	7.138	92% H-1→L
1C-c(c)	$S_0 \rightarrow S_1$	417	2.97	6.22	0.453	5.795	95% H→L
	$S_0 \rightarrow S_2$	384	3.23	4.41	0.349	5.696	97% H→L+1
	$S_0 \rightarrow S_3$	315	3.94	4.26	0.412	6.639	93% H-1→L
2C-c(t)	$S_0 \rightarrow S_1$	358	3.47	10.88	0.924	3.587	81% H→L+1, 15% H-1→L
	$S_0 \rightarrow S_2$	353	3.51	6.27	0.539	3.142	94% H→L
	$S_0 \rightarrow S_3$	345	3.60	1.88	0.166	6.201	78% H-1→L, 16% H→L+1
2C-c(c)	$S_0 \rightarrow S_1$	364	3.41	9.58	0.799	3.573	79% H→L+1, 17% H-1→L
	$S_0 \rightarrow S_2$	355	3.49	7.24	0.619	2.969	92% H→L
	$S_0 \rightarrow S_3$	349	3.56	1.40	0.122	6.168	76% H-1→L, 18% H→L+1
1D-ct	$S_0 \rightarrow S_1$	430	2.88	10.83	0.765	7.080	91% H→L
	$S_0 \rightarrow S_2$	388	3.19	6.88	0.539	7.310	91% H→L+1
	$S_0 \rightarrow S_3$	344	3.60	3.08	0.272	9.270	89% H-1→L
	$S_0 \rightarrow S_4$	327	3.79	1.48	0.138	10.207	80% H-1→L+1, 5% H-7→L+1
1D-cc	$S_0 \rightarrow S_1$	423	2.93	10.48	0.752	7.160	90% H→L
	$S_0 \rightarrow S_2$	384	3.23	6.49	0.513	7.364	91% H→L+1
	$S_0 \rightarrow S_3$	340	3.65	3.01	0.269	9.366	89% H-1→L

Table S2: continuation...

Comp.	Transition	λ_{ge}	ΔE_{ge}	μ^2_{ge}	f_{ge}	$\Delta\mu_{ge}$	Electronic excitations
1D-tt-ct	$S_0 \rightarrow S_4$	324	3.83	1.45	0.138	10.125	79% H-1→L+1, 6% H-7→L+1, 6% H-8→L+1
	$S_0 \rightarrow S_1$	419	2.96	7.87	0.571	7.941	90% H→L
	$S_0 \rightarrow S_2$	383	3.24	7.78	0.617	8.663	91% H→L+1
	$S_0 \rightarrow S_3$	343	3.61	5.02	0.444	10.483	90% H-1→L
	$S_0 \rightarrow S_4$	327	3.79	0.61	0.056	12.304	82% H-1→L+1
2D-ct	$S_0 \rightarrow S_1$	395	3.14	12.48	0.960	6.748	51% H-1→L, 41% H→L+1
	$S_0 \rightarrow S_2$	379	3.27	12.43	0.988	5.732	85% H→L, 9% H-1→L+1
	$S_0 \rightarrow S_3$	359	3.46	0.04	0.004	8.005	50% H→L+1, 39% H-1→L
1E-ct(t)	$S_0 \rightarrow S_1$	462	2.68	13.26	0.871	8.029	88% H→L
	$S_0 \rightarrow S_2$	410	3.02	8.13	0.602	8.061	87% H→L+1
	$S_0 \rightarrow S_3$	373	3.32	2.23	0.181	10.595	87% H-1→L
	$S_0 \rightarrow S_4$	352	3.52	1.87	0.161	11.850	83% H-1→L+1, 5% H→L
1E-tt(t)	$S_0 \rightarrow S_1$	447	2.77	9.24	0.627	9.425	87% H→L, 5% H-1→L+1
	$S_0 \rightarrow S_2$	403	3.08	9.82	0.740	9.895	86% H→L+1
	$S_0 \rightarrow S_3$	372	3.34	4.30	0.352	12.437	87% H-1→L
	$S_0 \rightarrow S_4$	350	3.54	0.65	0.056	14.636	84% H-1→L+1, 6% H→L
2E-ct(t)	$S_0 \rightarrow S_1$	427	2.91	12.82	0.913	8.920	58% H-1→L, 33% H→L+1
	$S_0 \rightarrow S_2$	404	3.07	14.33	1.078	7.702	82% H→L, 11% H-1→L+1
	$S_0 \rightarrow S_3$	378	3.28	0.23	0.018	9.681	57% H→L+1, 32% H-1→L
	$S_0 \rightarrow S_4$	353	3.51	0.66	0.057	11.805	83% H-1→L+1, 11% H→L
2E-ct(c)	$S_0 \rightarrow S_1$	436	2.84	14.14	0.985	8.807	60% H-1→L, 32% H→L+1
	$S_0 \rightarrow S_2$	411	3.01	14.17	1.046	7.519	82% H→L, 11% H-1→L+1
	$S_0 \rightarrow S_3$	384	3.23	0.27	0.021	9.674	59% H→L+1, 31% H-1→L
	$S_0 \rightarrow S_4$	359	3.45	0.63	0.053	11.633	83% H-1→L+1, 11% H→L
2E-cc(t)	$S_0 \rightarrow S_1$	424	2.93	12.50	0.896	9.136	58% H-1→L, 33% H→L+1
	$S_0 \rightarrow S_2$	401	3.09	14.61	1.108	7.810	81% H→L, 11% H-1→L+1
	$S_0 \rightarrow S_3$	376	3.29	0.20	0.017	9.750	57% H→L+1, 32% H-1→L
	$S_0 \rightarrow S_4$	351	3.53	0.57	0.049	12.116	83% H-1→L+1, 11% H→L

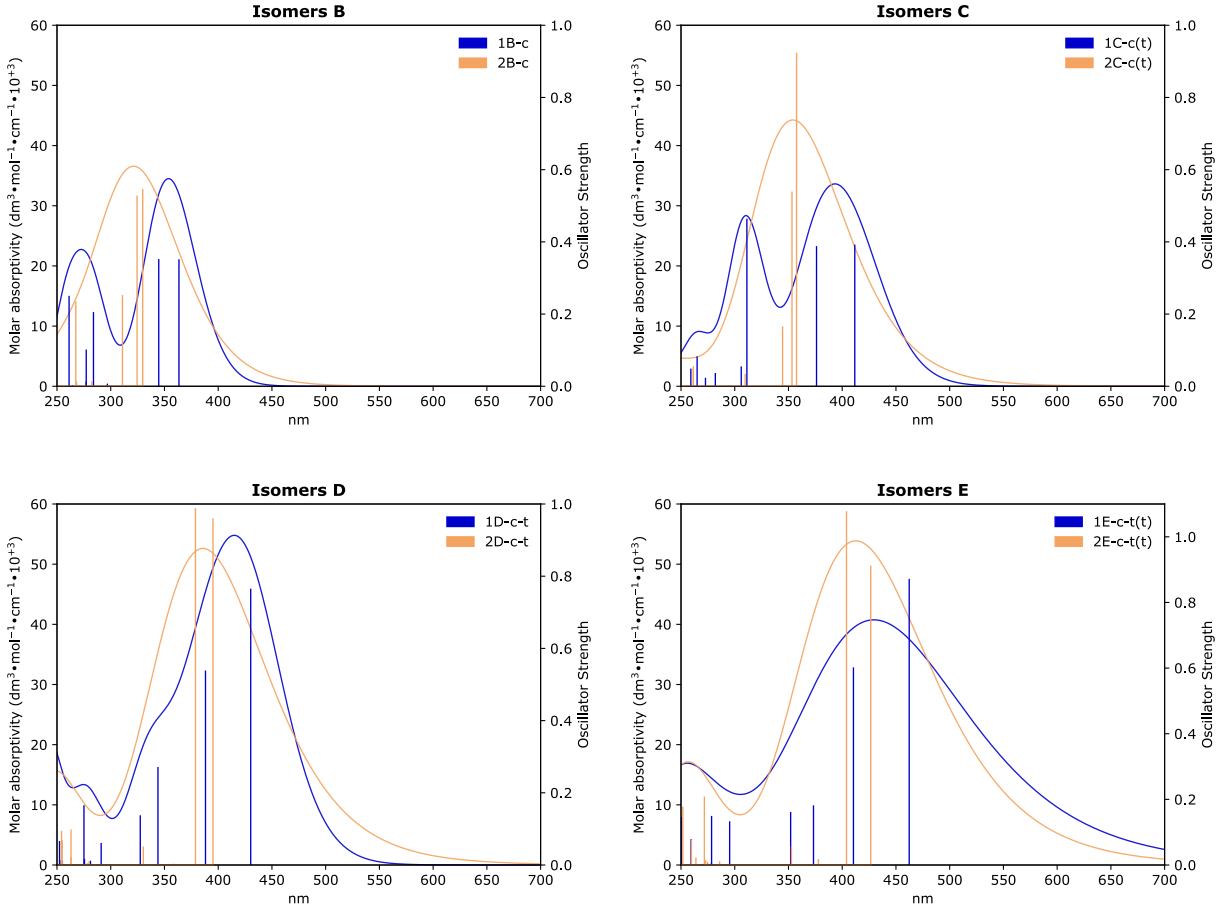

Figure S8: Calculated UV-vis spectra of the most stable conformers of Family 1 (blue) and Family 2 (orange) for isomers **B**, **C**, **D**, and **E**, as obtained at the IEF-PCM/M06-2X(D3)/6-311+G(d) level of theory in chloroform and using a Gaussian broadening of the absorption peaks (shown with the associated oscillator strengths) with a half-width at half-maximum (HWHM) of 0.25 eV.

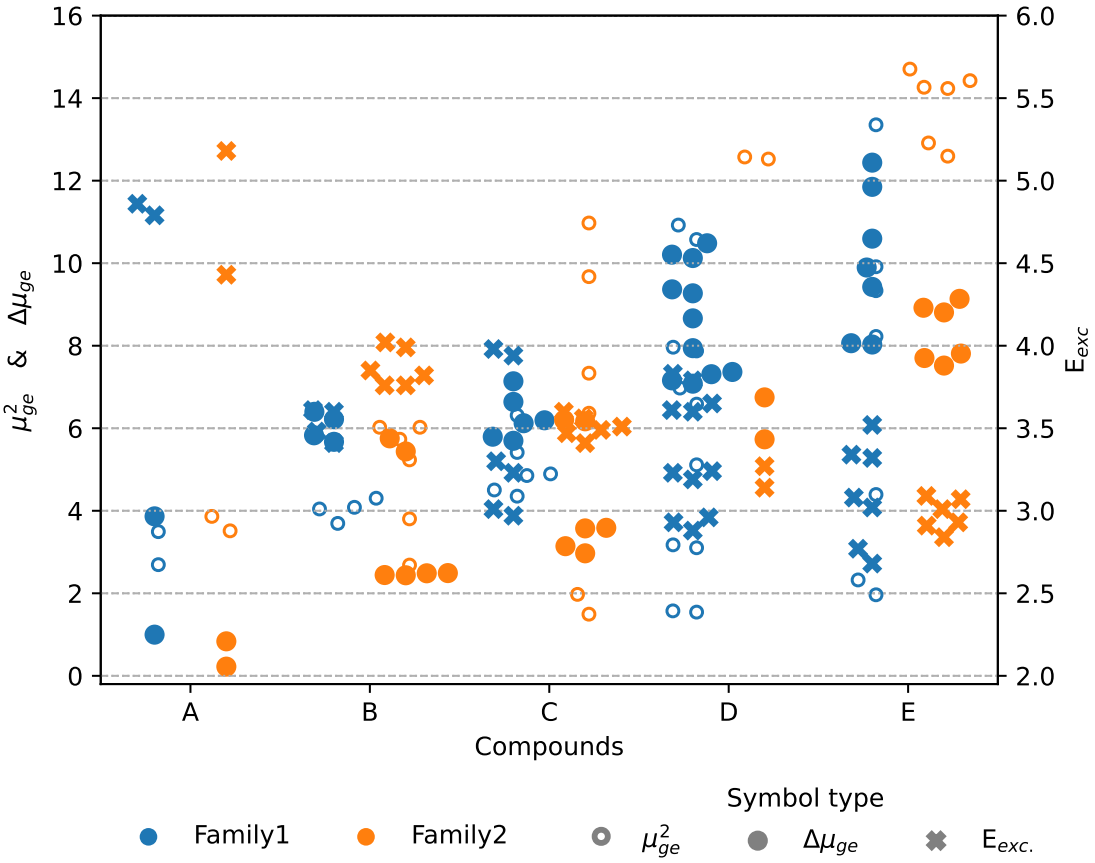

Figure S9: Summary-figure of the linear optical properties of the stable conformers for the two families of chromophores: squared transition dipoles ($\vec{\mu}_{ge}^2$, a.u.^{2}, empty circles), dipole moment differences ($\Delta\vec{\mu}_{ge}$, a.u., filled circles), and excitation energies ($E_{exc.}$, eV, cross marks). The two families of compounds are distinguished by the color code.

S4.1 Rationalization of the different energy splitting between $S_0 \rightarrow S_1$ and $S_0 \rightarrow S_2$ transitions for the two families of compounds

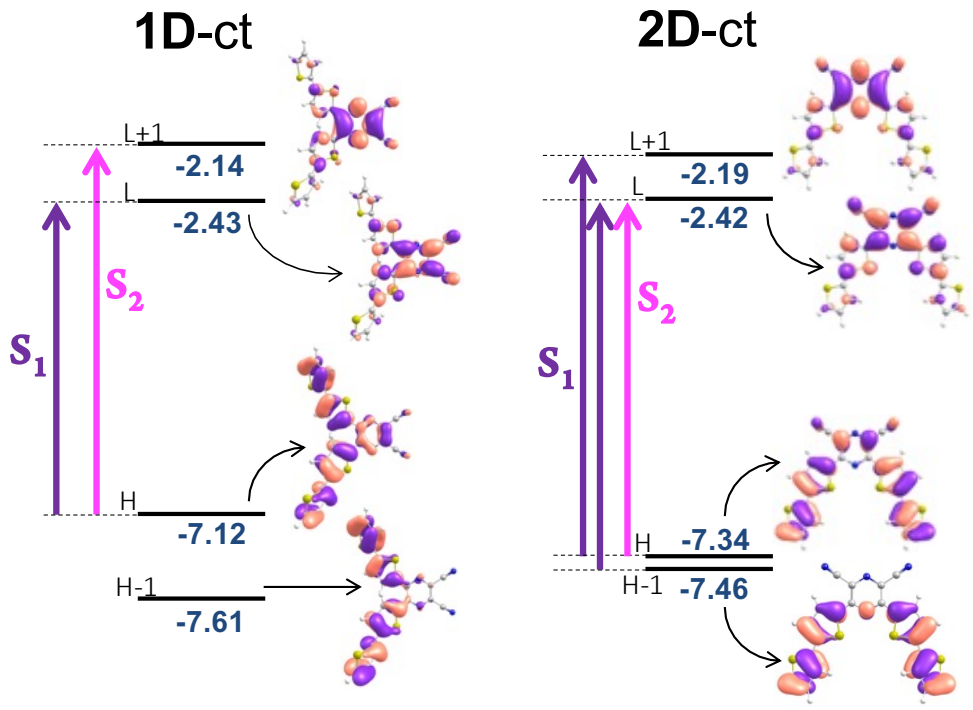

Figure S10: MO diagrams of isomers **1D**-ct and **2D**-ct. The main excitations that characterize the $S_0 \rightarrow S_1$ and $S_0 \rightarrow S_2$ transitions are represented in purple and pink, respectively. See Table S2 for further details. MO energies in eV.

Molecular orbital (MO) energies and gaps can be used to rationalize the higher splitting between the $S_0 \rightarrow S_1$ and $S_0 \rightarrow S_2$ electronic transitions observed for Family1 (see Figure S8). As it can be seen in Figure S10, the higher occupied orbitals (H and H-1) mainly involve the branches of the donor (D) substituents, and their energy gap can be directly related to the D-D interactions. Whereas, L and L+1 mainly involve the pyrazine, and their energy gap can be directly related to the substituents' and Ns' pattern within the pyrazine ring.

If we compare the main excitations that characterize the $S_0 \rightarrow S_1$ and $S_0 \rightarrow S_2$ transitions for each isomer, we can conclude that the energy gap between these electronic transitions will be mainly dictated by the L / L+1 and H / H-1 energy differences. For Family2, here exemplified with isomer **2D**-ct, these energy gaps are smaller than for Family1. This is

specially evident for the H / H-1 gap, indicating that there is a lower interaction between D groups, but also for the L / L+1 gap, which accounts for a different pattern in the pyrazine ring.

S5 NLO properties

S5.1 Expression of the $\langle\beta^2_{ZZZ}\rangle$ and $\langle\beta^2_{ZXX}\rangle$ invariants

The $\langle\beta^2_{ZZZ}\rangle$ and $\langle\beta^2_{ZXX}\rangle$ invariants (equations 5 and 6) have been calculated using the molecular β tensor components as follows:

$$\begin{aligned}\langle\beta^2_{ZZZ}\rangle = &\frac{1}{7}\sum_{\zeta}^{x,y,z}\beta^2_{\zeta\zeta\zeta} + \frac{4}{35}\sum_{\zeta\neq\eta}^{x,y,z}\beta^2_{\zeta\zeta\eta} + \frac{2}{35}\sum_{\zeta\neq\eta}^{x,y,z}\beta_{\zeta\zeta\zeta}\beta_{\zeta\eta\eta} \\ &+ \frac{4}{35}\sum_{\zeta\neq\eta}^{x,y,z}\beta_{\eta\zeta\zeta}\beta_{\zeta\zeta\eta} + \frac{4}{35}\sum_{\zeta\neq\eta}^{x,y,z}\beta_{\zeta\zeta\zeta}\beta_{\eta\eta\zeta} + \frac{1}{35}\sum_{\zeta\neq\eta}^{x,y,z}\beta^2_{\eta\zeta\zeta} \\ &+ \frac{4}{105}\sum_{\zeta\neq\eta\neq\xi}^{x,y,z}\beta_{\zeta\zeta\eta}\beta_{\eta\xi\xi} + \frac{1}{105}\sum_{\zeta\neq\eta\neq\xi}^{x,y,z}\beta_{\eta\zeta\zeta}\beta_{\eta\xi\xi} \\ &+ \frac{4}{105}\sum_{\zeta\neq\eta\neq\xi}^{x,y,z}\beta_{\zeta\zeta\eta}\beta_{\xi\xi\eta} \\ &+ \frac{2}{105}\sum_{\zeta\neq\eta\neq\xi}^{x,y,z}\beta^2_{\zeta\eta\xi} + \frac{4}{105}\sum_{\zeta\neq\eta\neq\xi}^{x,y,z}\beta_{\zeta\eta\xi}\beta_{\eta\zeta\xi}\end{aligned} \tag{S5}$$

$$\begin{aligned}\langle\beta^2_{ZXX}\rangle = &\frac{1}{35}\sum_{\zeta}^{x,y,z}\beta^2_{\zeta\zeta\zeta} + \frac{4}{105}\sum_{\zeta\neq\eta}^{x,y,z}\beta_{\zeta\zeta\zeta}\beta_{\zeta\eta\eta} - \frac{2}{35}\sum_{\zeta\neq\eta}^{x,y,z}\beta_{\zeta\zeta\zeta}\beta_{\eta\eta\zeta}\\ &+ \frac{8}{105}\sum_{\zeta\neq\eta}^{x,y,z}\beta^2_{\zeta\zeta\eta} + \frac{3}{35}\sum_{\zeta\neq\eta}^{x,y,z}\beta^2_{\zeta\eta\eta} - \frac{2}{35}\sum_{\zeta\neq\eta}^{x,y,z}\beta_{\zeta\zeta\eta}\beta_{\eta\zeta\zeta}\\ &+ \frac{1}{35}\sum_{\zeta\neq\eta\neq\xi}^{x,y,z}\beta_{\zeta\eta\eta}\beta_{\zeta\xi\xi} - \frac{2}{105}\sum_{\zeta\neq\eta\neq\xi}^{x,y,z}\beta_{\zeta\zeta\xi}\beta_{\eta\eta\xi}\\ &- \frac{2}{105}\sum_{\zeta\neq\eta\neq\xi}^{x,y,z}\beta_{\zeta\zeta\eta}\beta_{\eta\xi\xi}\\ &+ \frac{2}{35}\sum_{\zeta\neq\eta\neq\xi}^{x,y,z}\beta^2_{\zeta\eta\xi} - \frac{2}{105}\sum_{\zeta\neq\eta\neq\xi}^{x,y,z}\beta_{\zeta\eta\xi}\beta_{\eta\zeta\xi}\end{aligned} \tag{S6}$$

S5.2 Hyper-Rayleigh Scattering data calculated in dichloromethane

Table S3: Static and dynamic Hyper-Rayleigh Scattering (HRS) data calculated at the IEF-PCM/M06-2X(D3)/6-311+G(d) level of theory in dichloromethane: first hyperpolarizability (β_{HRS}) and depolarization ratio (DR), and their analogs $\beta_{HRS}(C_{2v})$ and $DR(C_{2v})$ calculated using equations 8 and 9, respectively, considering an exact C_{2v} symmetry. The deviation of $\beta_{HRS}(C_{2v})$ and $DR(C_{2v})$ with respect to the full value is given in parenthesis. All β values are expressed in a.u.

Compounds	Static ($\lambda = \infty$)				Dynamic (λ =1064 nm)	
	β_{HRS}	DR	$\beta_{HRS}(C_{2v})$	DR(C_{2v})	β_{HRS}	DR
1A-(c)	614	4.78	613 (-0.3%)	4.72 (-1.3%)	548	4.94
2A-(c)	686	2.32	691 (+0.7%)	2.39 (+3.0%)	617	2.40
1B-c	2936	5.53	2959 (+0.8%)	5.74 (+3.8%)	3650	6.84
2B-c	3064	2.97	3084 (+0.7%)	3.07 (+3.4%)	3507	3.09
1C-c(t)	6109	5.21	6125 (+0.3%)	5.30 (+1.7%)	9291	6.18
2C-c(t)	6388	3.22	6392 (+0.1%)	3.24 (+0.6%)	8484	3.32
1D-ct	9442	4.51	9415 (-0.3%)	4.57 (+1.3%)	20016	4.83
1D-cc	8942	4.55	8962 (+0.2%)	4.61 (+1.3%)	18029	4.89
2D-ct	10672	3.98	10697 (+0.2%)	4.03 (+1.3%)	19420	4.10
1E-ct(t)	16062	4.15	15562 (-3.11%)	4.25 (+2.4%)	47804	4.10
1E-tt(t)	15265	5.58	13635 (-10.7%)	5.84 (+4.7%)	36966	6.04
2E-ct(t)	17574	4.49	17593 (+0.1%)	4.52 (+0.7%)	40618	4.60
2E-ct(c)	19925	4.31	19919 (-0.03%)	4.32 (+0.2%)	49247	4.39
2E-cc(t)	17299	4.78	17315 (+0.1%)	4.81 (+0.6%)	38531	4.86

S5.3 Static β_{zxx} and β_{zzz} components calculated with Coupled-Perturbed Kohn-Sham

Table S4: Static β_{zxx} and β_{zzz} components (a.u.) and R ratios calculated at the IEF-PCM/M06-2X/6-311+G(d) level in chloroform.

Compound	β_{zxx}	β_{zzz}	R
1A-(c)	664	586	1.13
2A-(c)	996	42	23.93
1B-c	2656	3594	0.74
1B-t-c	2296	3627	0.63
2B-c	4152	1094	3.80
2B-t-c	4149	874	4.75
1C-c(t)	6005	6658	0.90
1C-c(c)	6789	6294	1.08
2C-c(t)	8366	2788	3.00
2C-c(c)	8193	3306	2.48
1D-ct	10630	8472	1.25
1D-cc	9999	8140	1.23
1D-tt-ct	8230	10718	0.77
2D-ct	12878	7841	1.64
1E-ct(t)	18398	12525	1.47
1E-tt(t)	12417	17345	0.72
2E-ct(t)	19776	15590	1.27
2E-ct(c)	23064	16361	1.41
2E-cc(t)	18503	16699	1.11

S5.4 Derivation of the SOS expression of β_{zxx} and β_{zzz}

The general formula for calculating β by means of the SOS method is:

$$\beta_{ijk}(-(\omega_1+\omega_2);\omega_1,\omega_2) =$$
$$\sum_{e,e'\neq 0}\Bigg[\frac{\langle 0|\tilde{\mu}_i|e\rangle\langle e|\tilde{\mu}_j|e'\rangle\langle e'|\tilde{\mu}_k|0\rangle}{(\Delta E_{ge}-\hbar(\omega_1+\omega_2))(\Delta E_{ge'}-\hbar\omega_2)}+\frac{\langle 0|\tilde{\mu}_i|e\rangle\langle e|\tilde{\mu}_k|e'\rangle\langle e'|\tilde{\mu}_j|0\rangle}{\Delta E_{ge}-\hbar(\omega_1+\omega_2))(\Delta E_{ge'}-\hbar\omega_1)}+$$
$$\frac{\langle 0|\tilde{\mu}_j|e\rangle\langle e|\tilde{\mu}_i|e'\rangle\langle e'|\tilde{\mu}_k|0\rangle}{(\Delta E_{ge}+\hbar\omega_1)(\Delta E_{ge'}-\hbar\omega_2)}+\frac{\langle 0|\tilde{\mu}_j|e\rangle\langle e|\tilde{\mu}_k|e'\rangle\langle e'|\tilde{\mu}_i|0\rangle}{(\Delta E_{ge}+\hbar\omega_1)(\Delta E_{ge'}+\hbar(\omega_1+\omega_2))}+$$
$$\frac{\langle 0|\tilde{\mu}_k|e\rangle\langle e|\tilde{\mu}_i|e'\rangle\langle e'|\tilde{\mu}_j|0\rangle}{(\Delta E_{ge}+\hbar\omega_2)(\Delta E_{ge'}-\hbar\omega_1)}+$$
$$\frac{\langle 0|\tilde{\mu}_k|e\rangle\langle e|\tilde{\mu}_j|e'\rangle\langle e'|\tilde{\mu}_i|0\rangle}{(\Delta E_{ge}+\hbar\omega_2)(\Delta E_{ge'}+\hbar(\omega_1+\omega_2))}\Bigg] \quad \text{(S7)}$$

where 0 refers to the ground state, e and e' account for excited states, and $\tilde{\mu}_i = \hat{\mu}_i - \langle 0|\hat{\mu}_i|0\rangle$.

Considering:

- Static regime.
- The following simplification on $\tilde{\mu}_i$ that can be done in numerators:

  $\langle 0|\hat{\mu}_i - \langle 0|\hat{\mu}_i|0\rangle|e\rangle\langle e|\hat{\mu}_j - \langle 0|\hat{\mu}_j|0\rangle|e'\rangle\langle e'|\hat{\mu}_k - \langle 0|\hat{\mu}_k|0\rangle|0\rangle =$

  $(\langle 0|\hat{\mu}_i|e\rangle - \langle 0|\hat{\mu}_i|0\rangle\langle 0|e\rangle)(\langle e|\hat{\mu}_j|e'\rangle - \langle 0|\hat{\mu}_j|0\rangle\langle e|e'\rangle)(\langle e'|\hat{\mu}_k|0\rangle - \langle 0|\hat{\mu}_k|0\rangle\langle e'|0\rangle) =$

  $(\langle 0|\hat{\mu}_i|e\rangle)(\langle e|\hat{\mu}_j|e'\rangle - \delta_{ee'}\langle 0|\hat{\mu}_j|0\rangle)(\langle e'|\hat{\mu}_k|0\rangle)$

eq. S7 can be rewritten as:

$$\beta_{ijk}(0;0,0) =$$
$$\sum_{e\neq 0}\sum_{e'\neq 0}\frac{\langle 0|\hat{\mu}_i|e\rangle(\langle e|\hat{\mu}_j|e'\rangle-\delta_{ee'}\langle 0|\hat{\mu}_j|0\rangle)\langle e'|\hat{\mu}_k|0\rangle}{\Delta E_{ge}\Delta E_{ge'}}+\sum_{e\neq 0}\sum_{e'\neq 0}\frac{\langle 0|\hat{\mu}_i|e\rangle(\langle e|\hat{\mu}_k|e'\rangle-\delta_{ee'}\langle 0|\hat{\mu}_k|0\rangle)\langle e'|\hat{\mu}_j|0\rangle}{\Delta E_{ge}\Delta E_{ge'}}+$$
$$\sum_{e\neq 0}\sum_{e'\neq 0}\frac{\langle 0|\hat{\mu}_j|e\rangle(\langle e|\hat{\mu}_i|e'\rangle-\delta_{ee'}\langle 0|\hat{\mu}_i|0\rangle)\langle e'|\hat{\mu}_k|0\rangle}{\Delta E_{ge}\Delta E_{ge'}}+\sum_{e\neq 0}\sum_{e'\neq 0}\frac{\langle 0|\hat{\mu}_j|e\rangle(\langle e|\hat{\mu}_k|e'\rangle-\delta_{ee'}\langle 0|\hat{\mu}_k|0\rangle)\langle e'|\hat{\mu}_i|0\rangle}{\Delta E_{ge}\Delta E_{ge'}}+$$
$$\sum_{e\neq 0}\sum_{e'\neq 0}\frac{\langle 0|\hat{\mu}_k|e\rangle(\langle e|\hat{\mu}_i|e'\rangle-\delta_{ee'}\langle 0|\hat{\mu}_i|0\rangle)\langle e'|\hat{\mu}_j|0\rangle}{\Delta E_{ge}\Delta E_{ge'}}+$$
$$\sum_{e\neq 0}\sum_{e'\neq 0}\frac{\langle 0|\hat{\mu}_k|e\rangle(\langle e|\hat{\mu}_j|e'\rangle-\delta_{ee'}\langle 0|\hat{\mu}_j|0\rangle)\langle e'|\hat{\mu}_i|0\rangle}{\Delta E_{ge}\Delta E_{ge'}} \quad \text{(S8)}$$

According to the previous equation, the terms that define β_{ijk} values by means of the SOS formalism can be expressed as an $[e*e']$ matrix (Figure S11), where we can distinguish diagonal (also called vertical) and off-diagonal (also called cross-terms) elements.

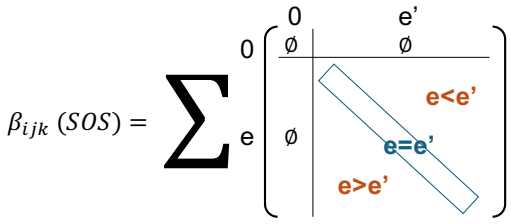

Figure S11: Matrix representation of the contributions that give β_{ijk} values according the SOS method.

Let's analyze eq. S8, splitting between diagonal and off-diagonal elements:

- $\underline{\mathbf{e} = \mathbf{e}'}$

$$\begin{aligned}
&\beta_{ijk}(-(0);0,0) = \\
&\sum_{e\neq 0} \frac{\langle 0|\hat{\mu}_i|e\rangle(\langle e|\hat{\mu}_j|e\rangle - \langle 0|\hat{\mu}_j|0\rangle)\langle e|\hat{\mu}_k|0\rangle}{\Delta E_{ge}\Delta E_{ge}} + \sum_{e\neq 0} \frac{\langle 0|\hat{\mu}_i|e\rangle(\langle e|\hat{\mu}_k|e\rangle - \langle 0|\hat{\mu}_k|0\rangle)\langle e|\hat{\mu}_j|0\rangle}{\Delta E_{ge}\Delta E_{ge}} + \\
&\sum_{e\neq 0} \frac{\langle 0|\hat{\mu}_j|e\rangle(\langle e|\hat{\mu}_i|e\rangle - \langle 0|\hat{\mu}_i|0\rangle)\langle e|\hat{\mu}_k|0\rangle}{\Delta E_{ge}\Delta E_{ge}} + \sum_{e\neq 0} \frac{\langle 0|\hat{\mu}_j|e\rangle(\langle e|\hat{\mu}_k|e\rangle - \langle 0|\hat{\mu}_k|0\rangle)\langle e|\hat{\mu}_i|0\rangle}{\Delta E_{ge}\Delta E_{ge}} + \\
&\sum_{e\neq 0} \frac{\langle 0|\hat{\mu}_k|e\rangle(\langle e|\hat{\mu}_i|e\rangle - \langle 0|\hat{\mu}_i|0\rangle)\langle e|\hat{\mu}_j|0\rangle}{\Delta E_{ge}\Delta E_{ge}} + \sum_{e\neq 0} \frac{\langle 0|\hat{\mu}_k|e\rangle(\langle e|\hat{\mu}_j|e\rangle - \langle 0|\hat{\mu}_j|0\rangle)\langle e|\hat{\mu}_i|0\rangle}{\Delta E_{ge}\Delta E_{ge}}
\end{aligned} \tag{S9}$$

$$\begin{aligned}
&\beta_{ijk}(-(0);0,0) = \\
&2\sum_{e\neq 0} \frac{\langle 0|\hat{\mu}_i|e\rangle\langle e|\hat{\mu}_k|0\rangle\Delta\hat{\mu}_j^{0e}}{\Delta E_{ge}\Delta E_{ge}} + 2\sum_{e\neq 0} \frac{\langle 0|\hat{\mu}_i|e\rangle\langle e|\hat{\mu}_j|0\rangle\Delta\hat{\mu}_k^{0e}}{\Delta E_{ge}\Delta E_{ge}} + 2\sum_{e\neq 0} \frac{\langle 0|\hat{\mu}_j|e\rangle\langle e|\hat{\mu}_k|0\rangle\Delta\hat{\mu}_i^{0e}}{\Delta E_{ge}\Delta E_{ge}}
\end{aligned} \tag{S10}$$

where $\Delta\hat{\mu}_i^{0e}$ accounts for the difference between permanent dipole moments of the ground state (0) and the excited state (e) into i direction.

- $\underline{\mathbf{e} \neq \mathbf{e}'}$

$$\beta_{ijk}(-(0);0,0) =$$
$$\sum_{\substack{e\neq 0\\ e}}\sum_{\substack{e'\neq 0\\ e'\neq e}} \frac{\langle 0|\hat{\mu}_i|e\rangle\langle e|\hat{\mu}_j|e'\rangle\langle e'|\hat{\mu}_k|0\rangle}{\Delta E_{ge}\Delta E_{ge'}} + \sum_{\substack{e\neq 0\\ e}}\sum_{\substack{e'\neq 0\\ e'\neq e}} \frac{\langle 0|\hat{\mu}_i|e\rangle\langle e|\hat{\mu}_k|e'\rangle\langle e'|\hat{\mu}_j|0\rangle}{\Delta E_{ge}\Delta E_{ge'}} +$$
$$\sum_{\substack{e\neq 0\\ e}}\sum_{\substack{e'\neq 0\\ e'\neq e}} \frac{\langle 0|\hat{\mu}_j|e\rangle\langle e|\hat{\mu}_i|e'\rangle\langle e'|\hat{\mu}_k|0\rangle}{\Delta E_{ge}\Delta E_{ge'}} + \sum_{\substack{e\neq 0\\ e}}\sum_{\substack{e'\neq 0\\ e'\neq e}} \frac{\langle 0|\hat{\mu}_j|e\rangle\langle e|\hat{\mu}_k|e'\rangle\langle e'|\hat{\mu}_i|0\rangle}{\Delta E_{ge}\Delta E_{ge'}} +$$
$$\sum_{\substack{e\neq 0\\ e}}\sum_{\substack{e'\neq 0\\ e'\neq e}} \frac{\langle 0|\hat{\mu}_k|e\rangle\langle e|\hat{\mu}_i|e'\rangle\langle e'|\hat{\mu}_j|0\rangle}{\Delta E_{ge}\Delta E_{ge'}} + \sum_{\substack{e\neq 0\\ e}}\sum_{\substack{e'\neq 0\\ e'\neq e}} \frac{\langle 0|\hat{\mu}_k|e\rangle\langle e|\hat{\mu}_j|e'\rangle\langle e'|\hat{\mu}_i|0\rangle}{\Delta E_{ge}\Delta E_{ge'}} \quad \text{(S11)}$$

since β_{ijk} is a diagonal matrix, we can write:

$$\beta_{ijk}(-(0);0,0) =$$
$$2\sum_{\substack{e\neq 0\\ e}}\sum_{\substack{e'\neq 0\\ e'>e}} \frac{\langle 0|\hat{\mu}_i|e\rangle\langle e|\hat{\mu}_j|e'\rangle\langle e'|\hat{\mu}_k|0\rangle}{\Delta E_{ge}\Delta E_{ge'}} + 2\sum_{\substack{e\neq 0\\ e}}\sum_{\substack{e'\neq 0\\ e'>e}} \frac{\langle 0|\hat{\mu}_i|e\rangle\langle e|\hat{\mu}_k|e'\rangle\langle e'|\hat{\mu}_j|0\rangle}{\Delta E_{ge}\Delta E_{ge'}} +$$
$$2\sum_{\substack{e\neq 0\\ e}}\sum_{\substack{e'\neq 0\\ e'>e}} \frac{\langle 0|\hat{\mu}_j|e\rangle\langle e|\hat{\mu}_i|e'\rangle\langle e'|\hat{\mu}_k|0\rangle}{\Delta E_{ge}\Delta E_{ge'}} + 2\sum_{\substack{e\neq 0\\ e}}\sum_{\substack{e'\neq 0\\ e'>e}} \frac{\langle 0|\hat{\mu}_j|e\rangle\langle e|\hat{\mu}_k|e'\rangle\langle e'|\hat{\mu}_i|0\rangle}{\Delta E_{ge}\Delta E_{ge'}} +$$
$$2\sum_{\substack{e\neq 0\\ e}}\sum_{\substack{e'\neq 0\\ e'>e}} \frac{\langle 0|\hat{\mu}_k|e\rangle\langle e|\hat{\mu}_i|e'\rangle\langle e'|\hat{\mu}_j|0\rangle}{\Delta E_{ge}\Delta E_{ge'}} + 2\sum_{\substack{e\neq 0\\ e}}\sum_{\substack{e'\neq 0\\ e'>e}} \frac{\langle 0|\hat{\mu}_k|e\rangle\langle e|\hat{\mu}_j|e'\rangle\langle e'|\hat{\mu}_i|0\rangle}{\Delta E_{ge}\Delta E_{ge'}} \quad \text{(S12)}$$

From the general expressions of diagonal (Equation S10) and off-diagonal elements (Equation S12), the corresponding expressions of β_{zzz} and β_{zxx} components can be derived from substitution:

- Diagonal elements. $\underline{\mathbf{e} = \mathbf{e}'}$

$$\beta_{zzz}(-(0);0,0) = 6\sum_{e\neq 0} \frac{\langle 0|\hat{\mu}_z|e\rangle\langle e|\hat{\mu}_z|0\rangle\Delta\hat{\mu}_z^{0e}}{\Delta E_{ge}\Delta E_{ge}} \quad \text{(S13)}$$

$$\beta_{zxx}(-(0);0,0) = 4\sum_{e\neq 0} \frac{\langle 0|\hat{\mu}_x|e\rangle\langle e|\hat{\mu}_z|0\rangle\Delta\hat{\mu}_x^{0e}}{\Delta E_{ge}\Delta E_{ge}} + 2\sum_{e\neq 0} \frac{\langle 0|\hat{\mu}_x|e\rangle\langle e|\hat{\mu}_x|0\rangle\Delta\hat{\mu}_z^{0e}}{\Delta E_{ge}\Delta E_{ge}} \quad \text{(S14)}$$

- Off-diagonal elements. $\underline{\mathbf{e} \neq \mathbf{e}'}$

$$\beta_{zzz}(-(0);0,0) = 12\sum_{\substack{e\neq 0\\ e}}\sum_{\substack{e'\neq 0\\ e'>e}} \frac{\langle 0|\hat{\mu}_z|e\rangle\langle e|\hat{\mu}_z|e'\rangle\langle e'|\hat{\mu}_z|0\rangle}{\Delta E_{ge}\Delta E_{ge'}} \tag{S15}$$

$$\begin{aligned}\beta_{zxx}(-(0);0,0) = 4\sum_{\substack{e\neq 0\\ e}}\sum_{\substack{e'\neq 0\\ e'>e}} \frac{\langle 0|\hat{\mu}_x|e\rangle\langle e|\hat{\mu}_x|e'\rangle\langle e'|\hat{\mu}_z|0\rangle}{\Delta E_{ge}\Delta E_{ge'}} + \\ 4\sum_{\substack{e\neq 0\\ e}}\sum_{\substack{e'\neq 0\\ e'>e}} \frac{\langle 0|\hat{\mu}_z|e\rangle\langle e|\hat{\mu}_x|e'\rangle\langle e'|\hat{\mu}_x|0\rangle}{\Delta E_{ge}\Delta E_{ge'}} + 4\sum_{\substack{e\neq 0\\ e}}\sum_{\substack{e'\neq 0\\ e'>e}} \frac{\langle 0|\hat{\mu}_x|e\rangle\langle e|\hat{\mu}_z|e'\rangle\langle e'|\hat{\mu}_x|0\rangle}{\Delta E_{ge}\Delta E_{ge'}}\end{aligned} \tag{S16}$$

S5.5 Calculation of transition electric dipole moments between excited states

Excited states $|e\rangle$ are expressed by linear combinations of singly excited Slater determinants (including excitations and deexcitations in the TD-DFT formalism):

$$|e\rangle = \sum_{i,a}\omega_{ia}|\Phi_i^a\rangle - \sum_{i,a}\omega'_{ia}|\Phi_i^a\rangle \tag{S17}$$

where $|\Phi_i^a\rangle$ is the spin-adapted configuration state function (CSF) in which an electron of the occupied molecular orbital (MO) ϕ_i is promoted to the virtual MO ϕ_a. ω_{ia} and ω'_{ia} are the corresponding variational coefficients for excitation and deexcitation processes, respectively.

The transition dipole moment between excited states K and L is defined as:

$$\langle K|\hat{\mu}|L\rangle = \sum_{i}^{occ}\sum_{a}^{vir}\omega_{i,a}^{K}\sum_{j}^{occ}\sum_{b}^{vir}\omega_{j,b}^{L}V^{iajb} + \sum_{i}^{occ}\sum_{a}^{vir}\omega_{i,a}^{\prime K}\sum_{j}^{occ}\sum_{b}^{vir}\omega_{j,b}^{\prime L}V^{iajb} \tag{S18}$$

with:

$$V^{iajb} = \begin{cases} \langle\phi_i|\hat{\mu}|\phi_a\rangle & (i=j, a\neq b) \\ -\langle\phi_i|\hat{\mu}|\phi_a\rangle & (i\neq j, a=b) \\ \mu^0 - \langle\phi_i|\hat{\mu}|\phi_i\rangle + \langle\phi_a|\hat{\mu}|\phi_a\rangle & (i=j, a=b) \\ 0 & (i\neq j, a\neq b) \end{cases} \tag{S19}$$

$$\mu^0 = \sum_{l}^{occ} \eta_l \langle \phi_l | \hat{\mu} | \phi_l \rangle \tag{S20}$$

where μ^0 corresponds to the ground state electric dipole moment with η being the orbital occupancy.

In practice, the MO and the excitation and deexcitation coefficients were calculated at the (TD)DFT level using Gaussian16 and provided as input for Multiwfn. To obtain accurate transition dipole moments, all monoelectronic transitions with configuration coefficients (ω_{ia}) larger than 10^{-5} have been considered in the excited state expression.

S5.6 Dipole and transition dipole moments of 1B-c and 2B-c

Dipole moments of 1B-c (a.u.)

i		j	Z	X	Y
0	--	0	4.5799883	0.0024800	-0.0003040
1	--	1	6.8737157	0.0023214	-0.0007082
2	--	2	6.8114709	0.0046821	0.0001967
3	--	3	4.8161769	0.0019673	-0.0004721
4	--	4	6.9208910	0.0067674	-0.0004328
5	--	5	7.5929532	0.8452615	0.0547691
6	--	6	6.2008666	-0.8438844	-0.0553593
7	--	7	8.1271091	-0.0075544	-0.0022034
8	--	8	7.5750510	0.0088921	0.0012591

Transition dipole moments of 1B-c (a.u.)

i		j	Z	X	Y
0	--	1	0.0045425	2.0425028	0.2034854
0	--	2	-1.9985722	0.0031230	0.0006973
0	--	3	-0.0024333	-0.1634675	-0.2137337
0	--	4	1.3858853	0.0067120	-0.0025479
0	--	5	-0.0547299	-0.9101148	0.3160253
0	--	6	-0.2495703	0.2305739	-0.0829720
0	--	7	-0.0086440	0.0076814	-0.1471194
0	--	8	-1.4690205	-0.0034668	0.0027160
1	--	2	0.0003243	0.4343126	0.1730546
1	--	3	-0.0930475	-0.0020743	-0.0003283
1	--	4	-0.0019721	2.3556787	0.3311802
1	--	5	0.1400392	-0.1970069	-0.0063747
1	--	6	-0.0330181	-0.8156391	-0.0291610

1	--	7	0.2675112	-0.0086144	-0.0016765
1	--	8	-0.0009014	-1.3040147	-0.2655472
2	--	3	0.0008610	0.5995837	0.1446198
2	--	4	0.0139608	-0.0007297	-0.0000793
2	--	5	-0.0155684	1.1700846	0.1601953
2	--	6	-0.0547283	-0.2935780	-0.0399441
2	--	7	-0.0006080	2.2411892	0.4521968
2	--	8	0.1557258	-0.0117686	-0.0026517
3	--	4	-0.0024398	0.4293785	0.1216710
3	--	5	0.3711456	-0.0088211	0.0263470
3	--	6	-0.0914181	-0.0418499	0.1040359
3	--	7	0.9530929	0.0049758	0.0001483
3	--	8	-0.0048588	0.6210879	0.0408829
4	--	5	-0.2771015	-0.7143313	0.0422820
4	--	6	-1.1036891	0.1721297	-0.0106414
4	--	7	-0.0013643	0.7174962	0.1273601
4	--	8	-0.4070320	0.0018907	-0.0000557
5	--	6	-0.4874776	1.9451189	0.0380388
5	--	7	0.1101523	-0.2942684	-0.0298756
5	--	8	-0.1745713	-1.1002271	0.0208555
6	--	7	-0.0290427	-1.1596274	-0.1216356
6	--	8	-0.6939214	0.2811909	-0.0049685
7	--	8	-0.0022903	-1.2555534	-0.2384175

Dipole moments of 2B-c (a.u.)

i		j	X	Z	Y
0	--	0	0.0000102	-3.1204199	-0.0000928
1	--	1	0.0000787	-4.1004017	-0.0001180
2	--	2	0.0000787	-4.0982377	-0.0000787
3	--	3	-0.0001574	-5.3851142	-0.0001180
4	--	4	0.0000000	-3.2850035	-0.0000787
5	--	5	-0.0000393	-5.6369261	-0.0001180
6	--	6	-0.0001180	-3.3823445	-0.0000787
7	--	7	0.0024394	-5.4302830	-0.0001180
8	--	8	-0.0023607	-5.3013081	-0.0000787

Transition dipole moments of 2B-c (a.u.)

i		j	X	Z	Y
0	--	1	-2.4364821	-0.0000862	0.0100789
0	--	2	0.0000909	-2.3752952	-0.0000074
0	--	3	-1.6094784	0.0000060	0.0058395
0	--	4	0.0185548	0.0000314	-0.1406531
0	--	5	-0.0000776	-0.3608386	-0.0000119

0	--	6	-0.0003168	0.0696568	-0.0000232
0	--	7	-0.0007548	-0.3441448	0.0000057
0	--	8	1.4381778	-0.0003227	0.0637182
1	--	2	-0.4338645	0.0000015	0.0235064
1	--	3	-0.0000235	-0.0781972	0.0000014
1	--	4	-0.0000345	0.0443888	0.0000164
1	--	5	-3.5306169	0.0000332	-0.0259144
1	--	6	-0.5514797	0.0000164	0.0083926
1	--	7	1.1092232	0.0002344	0.0215591
1	--	8	0.0000376	-0.3969454	0.0000088
2	--	3	-2.8784267	-0.0000081	-0.0276668
2	--	4	-0.1276866	0.0000140	0.0092342
2	--	5	0.0000012	-0.2578911	0.0000048
2	--	6	-0.0001621	0.0376882	-0.0000097
2	--	7	-0.0002062	-0.4505528	-0.0000011
2	--	8	0.5377914	-0.0002611	0.0254455
3	--	4	-0.0000207	-0.1031273	0.0000024
3	--	5	1.6674051	-0.0000153	0.0310706
3	--	6	0.3777807	0.0000596	0.0824921
3	--	7	-1.3108598	0.0002423	0.0161975
3	--	8	-0.0004417	-0.2653197	0.0000292
4	--	5	0.2066502	-0.0000140	0.0606412
4	--	6	0.5307667	-0.0000199	0.0394265
4	--	7	0.0086792	-0.0000995	-0.0105667
4	--	8	0.0000902	0.0840948	0.0000070
5	--	6	0.0002108	-0.3508591	-0.0000045
5	--	7	0.0007550	0.1173238	0.0000050
5	--	8	-1.3678887	-0.0006543	0.0062025
6	--	7	0.0003668	0.4715664	0.0000002
6	--	8	0.3016649	0.0004022	0.0046345
7	--	8	-3.0161778	0.0001987	0.0211561

References

(S1) Largent, R. J.; Polik, W. F.; Schmidt, J. R. Symmetrizer: Algorithmic determination of point groups in nearly symmetric molecules. *J. Comput. Chem.* **2012**, *33*, 1637–1642.